INCREASING IMAGING RESOLUTION BY COVERING YOUR SENSOR

Michael Schöberl[1], *Jürgen Seiler*[1], *Siegfried Foessel*[2], *and André Kaup*[1]

[1]Multimedia Communications and Signal Processing
University of Erlangen-Nuremberg
Cauerstr. 7, 91058 Erlangen, Germany

[2]Fraunhofer IIS
Am Wolfsmantel 33,
91058 Erlangen, Germany

ABSTRACT

Up to now, an increase in camera resolution required image sensors with more and more pixels. However, acquisition systems are limited in their pixels per second throughput given as power and complexity constraints. Simply capturing more pixels in a given system is often not possible. We propose a new non-regular imaging architecture that samples only few pixels and reconstructs a high resolution image afterwards. Our sampling is optimized to provide non-regular spatial sampling from a sensor with regular readout circuits. An existing slow image acquisition system can then be used to capture the data. The image reconstruction is performed with a local sparsity-based approach. The result is a high resolution image that requires a much smaller effort during acquisition.

Index Terms— Image Sensor, Digital Camera, Resolution Enhancement, Sparsity

1. INTRODUCTION

If the resolution of an image sensor is not sufficient for a certain application, one would usually replace the sensor (and lens) by higher resolution models. Unfortunately, the increase in sensor resolution directly increases the power consumption and cost of the system: More pixels need to be read out of the sensor array in the same amount of time, which requires more power. The A/D conversion needs to speed up and further components like storage, compression or image processing get much more complex.

As an alternative, the increase in resolution through image processing has been studied extensively for regular sampling: General interpolation algorithms (linear, bi-cubic, splines, ...) are widely used. Super resolution image reconstruction is typically based on displacement estimation, interpolation and deconvolution. Multiple low-resolution images of the same scene are required [1]. Single-image super resolution operates on a single low resolution image and performs reconstruction by comparison with image patches from a training set. A plausible creation of new high resolution image information can be achieved [2].

For non-regular sampling an increase in resolution can be gained through compressed sensing theory: A real world image can be described as a sparse signal in a transform domain and one can estimate the best fitting basis functions that generate a good image from only some of the samples. Image reconstruction for a regular sensor with a large number of unused pixels is shown in [3]. Compared to a high resolution sensor this does not save any readout time or power.

The paper is organized as follows: Sampling architectures are shown in the next Section. Our proposed sampling and image reconstruction are explained in Section 3 and 4. Simulation results and images are shown in Section 5.

2. SPATIAL DOMAIN IMAGE SAMPLING

Various methods for image sampling are shown in Fig. 1. If we had all the resources we want, the best option for high resolution images would be a high resolution sensor as shown in Fig. 1 a). However, a large number of rows and readout circuits requires a lot of time and power for reading all the pixels. For comparison, the low resolution sensor shown in Fig. 1 c) has only $1/4$ of the pixels with half the rows and half the readout circuits and is called "unshielded". A single image readout is faster and requires less power but will only yield low resolution images.

In practice, each pixel has only a certain area that is sensitive to light [4], while the remainder is taken up with transistors and wiring. An equivalent low resolution sensor with fill factor 25% is shown in Fig. 1 d). We call this sampling "$1/4$ regular".

Alternative systems have been proposed to enable the reconstruction of high resolution images from few samples. A regular image sensor with many unused pixels [3] is shown in Fig. 1 b). A random sampling is performed for subsequent reconstruction of high resolution images. Unfortunately, the readout circuits of the pixel array are not adapted to the randomness. The readout of good pixels also requires the readout of all unused samples. In this case 75 % of power or time would be wasted on reading unused samples and no advantage in power or frame rate is gained. The line buffer approach for random sampling in [5] is similar. All samples are available in memory and only random pixels are used in further processing. If we already have all the pixels, discarding and reconstruction can not increase image resolution. The overhead of reading and discarding pixels is only acceptable for a very low number of defect pixels. We show the application of sparsity-based defect interpolation on Bayer pattern raw data in [6].

3. PROPOSED SAMPLING

We propose an image sensor that performs non-regular spatial sampling as shown in Fig. 1 e). The sensor has regular large pixels, but the light sensitive area is placed differently for each pixel. The pixel area is divided into 4 quadrants and only one of them is sensitive to light. The result is a random sampling pattern on the high resolution grid. The underlying image sensor architecture (buses and readout circuitry) is still regular as with a regular low-resolution sensor.

A practical implementation can be created from off-the-shelf low-resolution image sensors with high fill factor (e.g. with microlenses). Additional shielding from light is applied on top of it. For each large pixel one of four possible masks needs to be applied randomly. It is also possible to design sensors based on four different pixel layouts where the light sensitive area is directly placed in one of the quadrants. Unfortunately, the systems from Fig. 1 b), d) and e) will have a fixed fill factor of only 25% and will have a reduced

978-1-4577-1302-6/11/$26.00 ©2011 IEEE

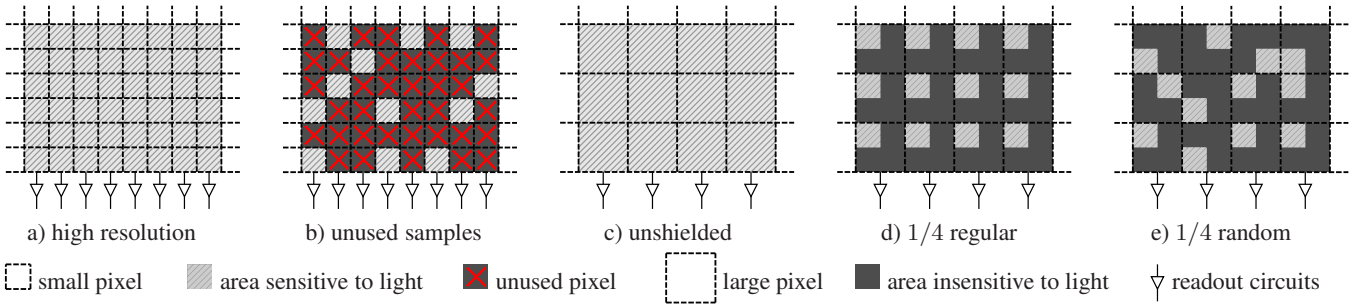

Fig. 1. Sampling patterns: a) high resolution sensor, b) high resolution sensor with 75% unused pixels [3] c) low resolution sensor, d) more realistic pixels with fill factor 25%, some parts are not sensitive to light and e) proposed non-regular placement of area sensitive to light

sensitivity compared to Fig. 1 a) and c). For now, only independent color channels as in 3-chip cameras are considered.

The resulting non-regular pattern is not truly random, as each large pixel we will have exactly one quadrant that is sensitive to light. For image reconstruction the next samples are always close. We believe that this is beneficial as natural images are non-stationary and a somewhat evenly distributed sampling is better for adjusting to changes in statistical properties of the image. Due to our block based reconstruction the pattern only needs to be uncorrelated in a nearby neighborhood. This can facilitate manufacturing. An enhancement in resolution of the whole system can only be gained if the optical path is able to deliver the resolution. The optical anti-alias filters need to match the high resolution sampling grid [4] and the lens needs to be good enough for the pixel size.

4. SPARSITY-BASED IMAGE RECONSTRUCTION

The reconstruction is carried out on blocks of size $M \times N$ pixels on the high resolution grid. The area to be reconstructed is located in the center and is of size $M_\mathrm{R} \times N_\mathrm{R}$. An exemplary block with $M \times N = 28 \times 28$ and $M_\mathrm{R} \times N_\mathrm{R} = 4 \times 4$ is shown in Fig. 3. The regarded block is called processing area $\mathcal{L}$ and is depicted by spatial coordinates m and n on the high resolution grid. Area $\mathcal{L}$ can be further divided in subareas as shown in Fig. 3 a): area $\mathcal{A}$ (white) holds all directly sampled pixels, area $\mathcal{B}$ (black) contains all unknown pixels and area $\mathcal{C}$ (gray) is used for previously reconstructed values. During the model generation, the weighting function

$$w'[m,n] = \begin{cases} 1 & \text{for } (m,n) \in \mathcal{A} \\ 0 & \text{for } (m,n) \in \mathcal{B} \\ \delta & \text{for } (m,n) \in \mathcal{C} \end{cases} \tag{1}$$

is used to weight each sample depending on its origin. The weight δ is used for previously processed pixels with processing in line-scan order as shown in Fig. 3 a). The influence of each sample depending on its position is further refined to

$$w[m,n] = w'[m,n] \cdot \hat{\rho}^{\sqrt{\left(m-\frac{M-1}{2}\right)^2+\left(n-\frac{N-1}{2}\right)^2}} \tag{2}$$

Thus, pixels far away from the center obtain a smaller weight and consequently less influence on the model generation. The weight of known samples decreases exponentially with increasing distance and is controlled by decay factor $\hat{\rho}$ as shown in Fig. 3 b).

For estimating the missing pixels, the complex-valued Frequency Selective Extrapolation (cFSE) from [7] is used. This algorithm iteratively generates the sparse model

$$g\,[m,n] = \sum_{(k,l)\in\mathfrak{K}} c_{(k,l)}\varphi_{(k,l)}\,[m,n] \tag{3}$$

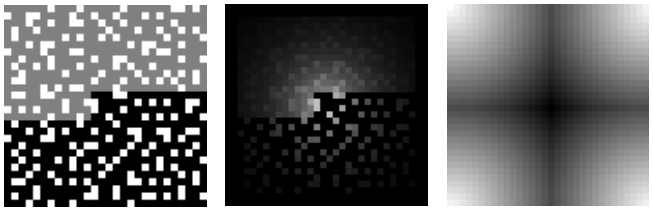

Fig. 3. Visualization of cFSE parameters: a) exemplary area $\mathcal{L}$ with division in subareas $\mathcal{A}$ (white), $\mathcal{B}$ (black) and $\mathcal{C}$ (gray), b) area $\mathcal{L}$ with weighting of pixels $w[m,n]$ and c) basis function probability $p[k,l]$ with high frequencies in the center

of the signal as weighted superposition of the two-dimensional basis functions $\varphi_{(k,l)}\,[m,n]$. The weights of the individual basis functions are controlled by the expansion coefficients $c_{(k,l)}$ and set $\mathfrak{K}$ holds the indices of all basis functions used for model generation. As proposed in [7] we use the functions of the two-dimensional discrete Fourier transform as basis functions. These functions enable cFSE to recover different image content like smooth as well as noise like areas and edges at high quality. Furthermore, the reconstruction can be carried out efficiently in the Fourier domain using a 2D-FFT of size $T \times T$. For generating the model, cFSE selects one basis function to be added to the model and estimates the corresponding weight in every iteration.

Unlike [7], the selection can be ambiguous due to the small number of available samples. To favor a smooth solution, we assign a linear decreasing probability $p[k,l]$ to basis functions with increasing frequency:

$$p[k,l] = \frac{1}{p_0}\left(1 - \frac{\sqrt{2}}{T}\sqrt{\tilde{k}^2+\tilde{l}^2}\right) \tag{4}$$

with $\tilde{k} = \frac{T}{2} - |k - \frac{T}{2}|$ and $\tilde{l} = \frac{T}{2} - |l - \frac{T}{2}|$ and p_0 is used for normalizing the sum over $p[k,l]$ to one. This replicates typical point spread functions from optical domain acquisition: The higher the frequency, the more of the signal will be attenuated [4]. An exemplary probability $p[k,l]$ is shown in Fig. 3 c) with the top left corner corresponding to DC index $[k,l] = [0,0]$.

The sparse model $g\,[m,n]$ is defined over the whole area $\mathcal{L}$. The center area of the generated model is finally used as the reconstructed signal. Due to this block based approach, the image reconstruction scales linearly with the total number of pixels and directly allows for excellent parallelization. For an extensive discussion and source code of cFSE, please refer to [7].

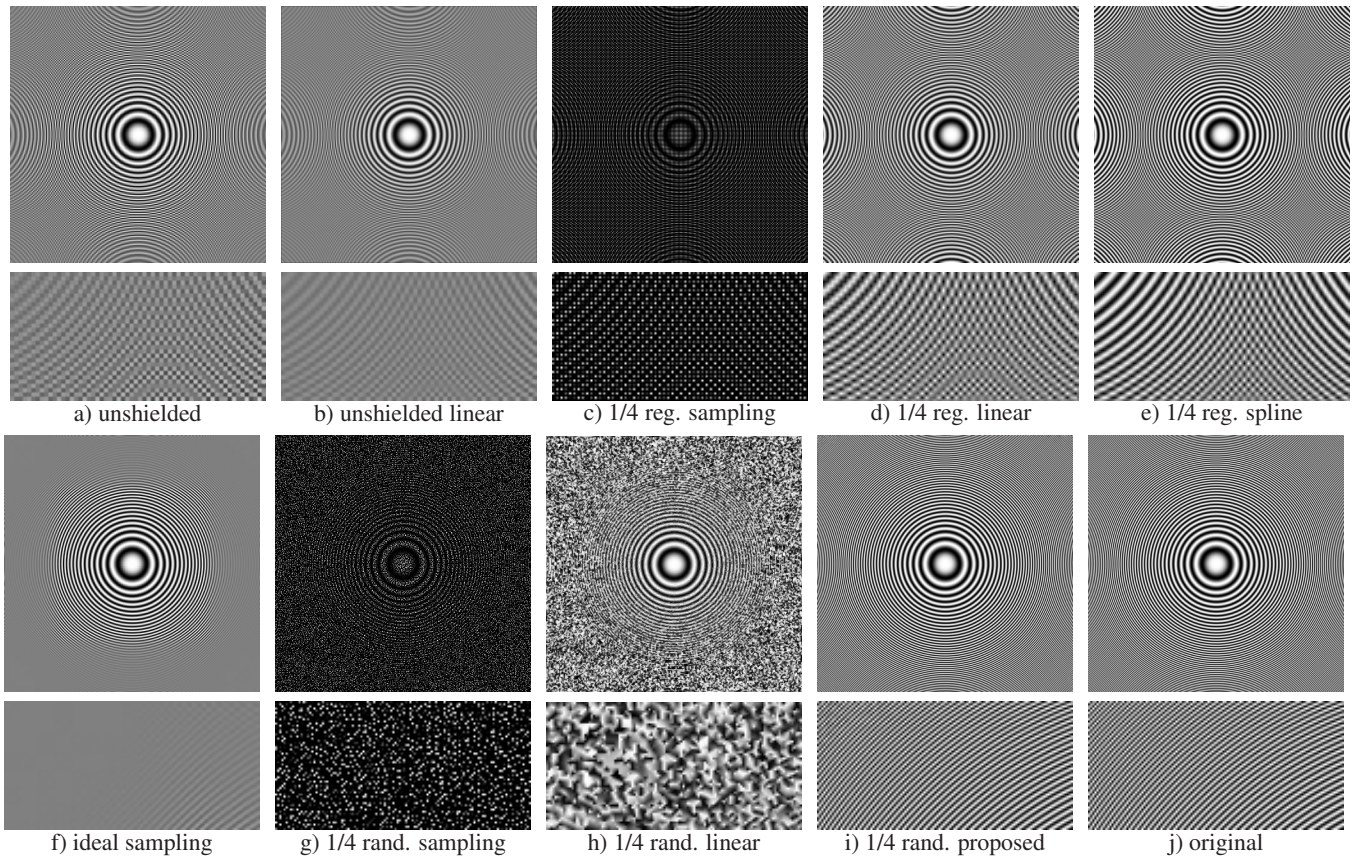

Fig. 2. Sampling for *Zone Plate* test pattern, full image (top) and cropped region (bottom): a) and c) show aliased sampling, b), d) and e) show linear, linear and spline based interpolation of a) and c), significant aliasing is visible, f) shows ideal sampling and interpolation, g) proposed $1/4$ random sampling, h) linear Delaunay interpolation of random sampling, i) proposed cFSE reconstruction of g) and j) original. *(Please pay attention, additional aliasing may be caused by printing or scaling! Best to be viewed enlarged on a monitor!)*

5. SIMULATION RESULTS

Our simulation compares the proposed non-regular sampling to regular low resolution sampling. Compared to the original image, the sampling for all methods uses $1/4$ of the samples according to Fig. 1 c) to e). Furthermore, ideal sampling with optimum low-pass filtering is considered. For comparison, image reconstruction for aliased sampling is carried out with linear and spline interpolation. The linear interpolation for non-regular sampling is based on Delaunay triangulation [8]. All operations are carried out in independent color channels (similar to a perfectly aligned 3-chip camera).

In our simulation we used the following parameters for cFSE: the area to be reconstructed is of size $M_{\mathrm{R}} \times N_{\mathrm{R}} = 4 \times 4$ with blocks of size $M \times N = 28 \times 28$, weight for previously processed samples $\delta = 0.75$, weight decay factor $\hat{\rho} = 0.7$, orthogonality correction $\gamma = 0.25$, maximum number of iterations $\nu_{\max} = 500$ and basis functions emanate from an FFT of size $T = 32$. For an extensive discussion of the parameters, please refer to [7].

Table 1 shows a PSNR comparison to the original high resolution image. For regular images like *Lighthouse* (Kodim19) and the *Zone Plate* we can get large gains compared to traditional sampling. For mostly random content like the hair of the woman in Kodim04 the reconstruction is difficult. In noise-like image regions a low-pass solution would be favored in terms of PSNR. As shown in [9] PSNR can only be used as a hint for evaluating visual quality. Still, the images reconstructed with our method are competitive.

Sampling	unshielded	$1/4$ regular		ideal	$1/4$ random	
Reconstruction	-	linear	linear	spline	ideal	linear	proposed
Kodim04	31.0	31.7	31.0	30.4	33.2	31.3	32.4 dB
Kodim08	22.4	22.6	22.3	21.7	23.9	21.8	24.2 dB
Kodim19	27.0	27.0	27.1	26.7	28.6	26.2	30.0 dB
Zone Plate	11.1	10.7	10.4	9.3	11.2	9.5	38.9 dB

Table 1. PSNR results for different samplings and reconstruction

The *Zone Plate* test pattern with different sampling patterns is shown in Fig. 2. This 2D chirp signal contains all frequencies. Directly sampling the high resolution with few regular samples leads to aliasing as shown in Fig. 2 a) and c). Neither linear nor spline based interpolation can remove this any more as shown in Fig. 2 b), d) and e). Ideal sampling and interpolation in Fig. 2 f) does not produce aliasing but loses all high frequencies. The proposed random sampling is shown Fig. 2 g). The non-regular linear interpolation is not able to recover high frequencies as shown in Fig. 2 h). Our proposed cFSE reconstruction in i) is able to fully reconstruct all image detail and all frequencies of the original image can be recovered. Compared to the original in Fig. 2 j) no difference is visible.

For natural images the improved reconstruction quality is shown in Fig. 4. Independently from image characteristics we can generate a high visual quality compared to the results from traditional sampling. For structured images like *Lighthouse* (Kodim19) a very good reconstruction of details is possible. Even in random textures like in Kodim04 a visually appealing reconstruction can be obtained.

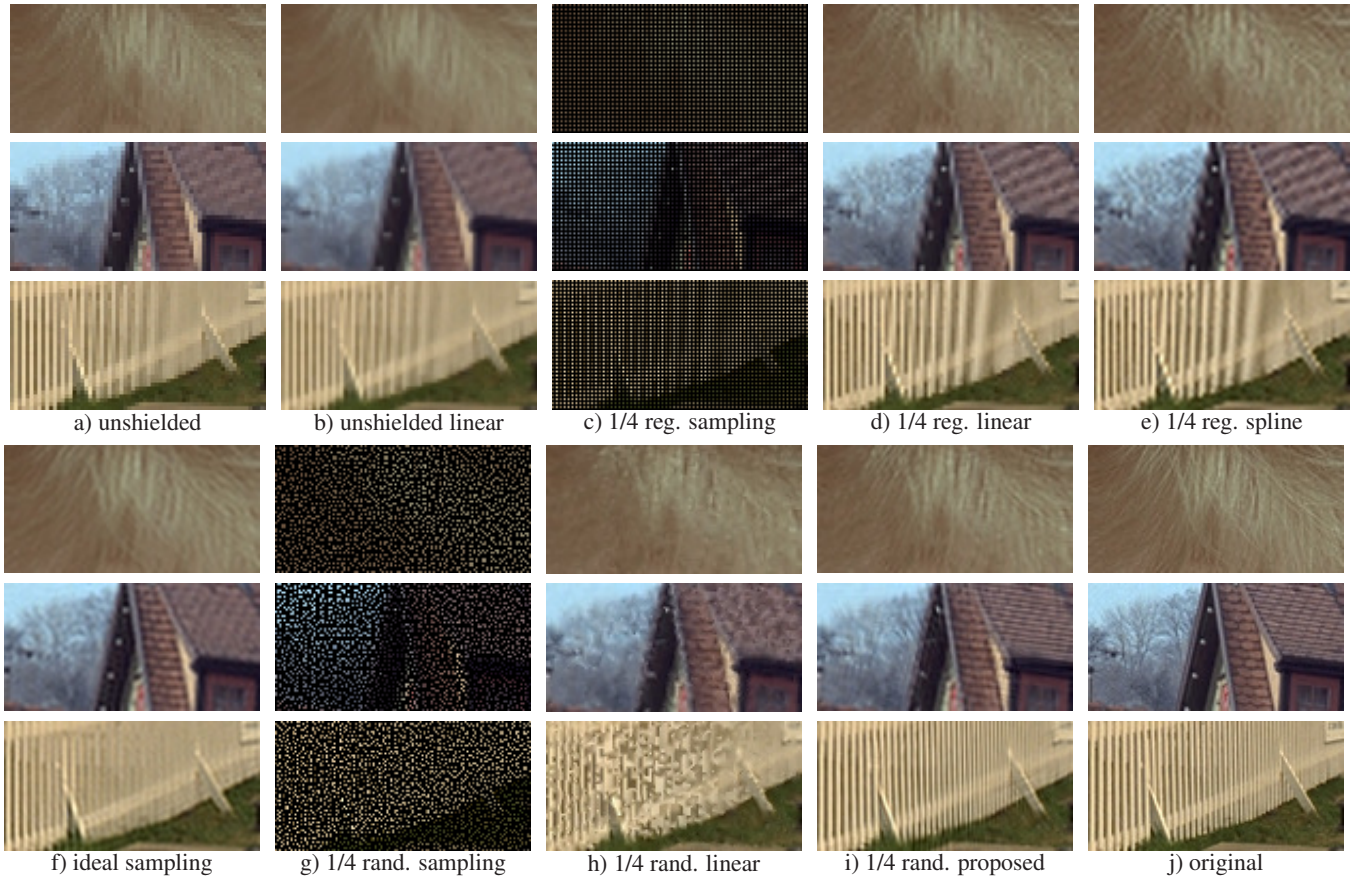

Fig. 4. Cropped examples from Kodak image set, Kodim04 (top), Kodim08 (middle) and Kodim19 (bottom), see Fig. 2 and text. Good reconstruction in structured areas and plausible image content in random textures for proposed method in i)

6. CONCLUSION

We presented a novel approach to non-regular sampling and image reconstruction. We shield parts of each pixel of a regular low resolution image sensor. This gives a non-regular sampling pattern that can be read out of the sensor with low effort. We then reconstruct high resolution image details based on the sparsity assumption with an iterative block based algorithm in the Fourier domain. Our results show that this works excellent for structured image regions and still generates plausible images for random textures. The result is an increase in resolution by shielding parts of the pixels of a low resolution sensor. A high resolution camera does not require high resolution sensors any more. During acquisition we can now save power, complexity and cost. Additional processing is required for high resolution image reconstruction.

7. REFERENCES

[1] S.C. Park, M.K. Park, and M.G. Kang, "Super-resolution image reconstruction: a technical overview," *IEEE Signal Processing Magazine*, vol. 20, no. 3, pp. 21 – 36, May 2003.

[2] W.T. Freeman, T.R. Jones, and E.C. Pasztor, "Example-based super-resolution," *IEEE Computer Graphics and Applications*, vol. 22, no. 2, pp. 56 –65, 2002.

[3] P. Sen and S. Darabi, "A novel framework for imaging using compressed sensing," in *IEEE International Conference on Image Processing (ICIP)*, nov. 2009, pp. 2133 –2136.

[4] M. Schöberl, W. Schnurrer, A. Oberdörster, S. Fößel, and A. Kaup, "Dimensioning of optical birefringent anti-alias filters for digital cameras," in *IEEE International Conference on Image Processing (ICIP)*, Hong Kong, Sept. 2010, pp. 3457–3460.

[5] C.H. Lin and K. Chin, "Pixel-data line buffer approach having variable sampling patterns," July 6 2010, US Patent 7,750,979.

[6] M. Schöberl, J. Seiler, B. Kasper, S. Fößel and A. Kaup, "Sparsity-based defect pixel compensation for arbitrary camera raw images," in *accepted for IEEE International Conference on Acoustics, Speech, and Signal Processing (ICASSP)*, Prague, Czech Repubic, May 2011.

[7] J. Seiler and A. Kaup, "Complex-valued frequency selective extrapolation for fast image and video signal extrapolation," *IEEE Signal Processing Letters*, vol. 17, no. 11, pp. 949 –952, Nov. 2010.

[8] B. Delaunay, "Sur la sphère vide [On the empty area]," *Izvestia Akademii Nauk SSSR, Otdelenie Matematicheskikh i Estestvennykh Nauk*, vol. 7, pp. 793–800, 1934.

[9] Z. Wang and A.C. Bovik, "Mean squared error: Love it or leave it? a new look at signal fidelity measures," *IEEE Signal Processing Magazine*, vol. 26, no. 1, pp. 98 –117, 2009.